

## Interaction of Hysteretic Behavior between Isolator/Damper and Pier in an Isolated Bridge

Kazuhiko Kawashima\* and Gaku Shoji\*\*

\*Dr. of Eng. , Professor, Department of Civil Engineering, Tokyo Institute of Technology, 2-12-1,  
O-okayama, Meguro-ku, Tokyo 152

\*\*M. of Eng. , Research Associate Department of Civil Engineering, Tokyo Institute of Technology, 2-12-1,  
O-okayama, Meguro-ku, Tokyo 152

Because nonlinear hysteretic response occurs in both the isolator / damper and the pier in an isolated bridge subjected to an extreme ground motion, there must be an interaction between the device and the pier. This paper presents an analysis on the interaction with emphasis on the yield force level of the device and the elongation of natural period required for the seismic isolation bridges.

*Key Words:* bridges, seismic design, menshin bridge, nonlinear hysteretic response

### 1. Introduction

Since the 1995 Hyogo-ken Nanbu earthquake, the Menshin design (seismic isolation) has been extensively adopted for new bridge construction. The technical development which was compiled in a form of the "Guidelines of Menshin Design of Highway Bridges" in 1989<sup>1)</sup> and the "Manual of Menshin Design of Highway Bridges" in 1993<sup>2),3)</sup> has been effectively used. The Menshin design was included in the Design Specifications of Highway Bridges revised in 1996<sup>4)</sup>. It was the first time that the Menshin design was incorporated in a code of bridges.

The Menshin design is the seismic isolation with the limited increase of natural period by placing emphasis on the increase of energy dissipation and the distribution of lateral force to as many substructures as possible<sup>2),5)</sup>. The slightly distorted application of the seismic isolation has been adopted in Japan, because significant increase of the natural period causes the increase of deck displacement<sup>5)</sup>. This requires to either adopt large expansion joints or accept large pounding force at joints. Soil condition is generally weaker in Japan than other countries. Large ground motions induced by the subduction-type fault earthquake with magnitude as large as 8 could result in the ground motions with predominant long period component. Thus, it is recommended in the Design Specifications of Highway Bridges that excessive elongation of natural period should not be made, and that the natural period of a menshin bridge may be less than about 2 times the natural period of the same bridge supported by the conventional bearings. This is one of the requirement for the minimum stiffness and the yielding force in the design of the isolator/energy

dissipator.

It is ideal in an isolated bridge that the energy is dissipated only at the device so that the substructure does not cause any hysteretic response during a design earthquake<sup>6),7)</sup>. However, in the Menshin design concept, it is not feasible that the menshin bridge responses with energy dissipation only at the device when the bridge is subjected to an extreme earthquake. Hysteretic response therefore occurs at the pier as well as the device. Thus, nonlinear interaction between the piers and the devices should be carefully considered in the design of the isolated bridge.

This paper discusses an analysis of the nonlinear response of bridges with hysteresis behavior at both the pier and the device with an emphasis on the effect of yielding force level and the post-yielding stiffness of the device.

### 2. Analytical Model and Analytical Conditions

In an isolated bridge, the response displacement at the gravity center of the deck  $u_D$  may be represented as (refer to Fig. 1)

$$u_D = u_F + H\theta_F + (H - H_f - \frac{L_P}{2})\theta_P + u_{PB} + u_B \quad (1)$$

in which  $u_F$  and  $\theta_F$  : translation and rotation of the footing,  $\theta_P$  : plastic rotation at plastic hinge of a pier,  $u_{PB}$  : flexural deformation of a pier,  $u_B$  : displacement of the device,  $H$  : distance from the bottom of the pier to the gravity center of the deck,  $H_f$  : height of the footing and  $L_P$  : plastic hinge length.

The lateral force vs. lateral displacement relation of the pier and the device may be represented as shown in Figs. 2

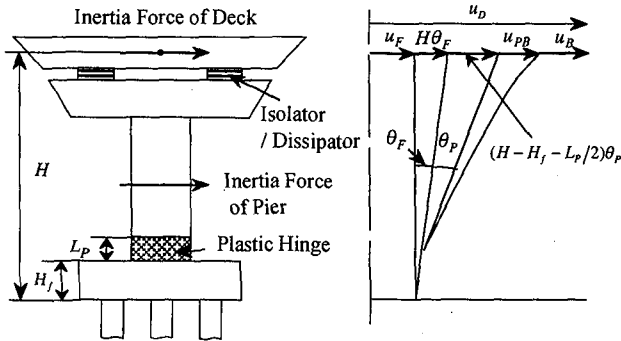


Fig. 1 Deformation of an Isolated Bridge

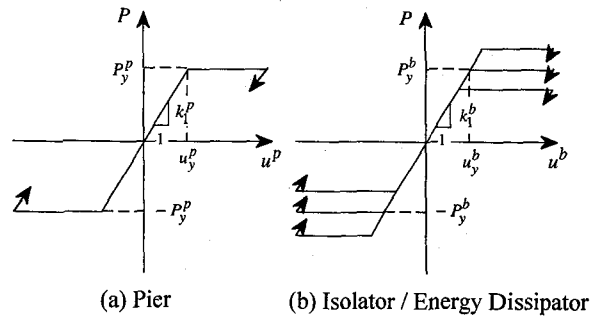


Fig. 2 Hysteresis Behavior of Pier and Device with Zero Post-Yield Stiffness

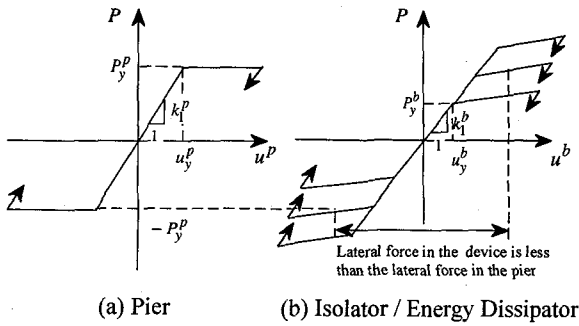


Fig. 3 Hysteresis Behavior of Pier and Device with Positive Post-Yield Stiffness

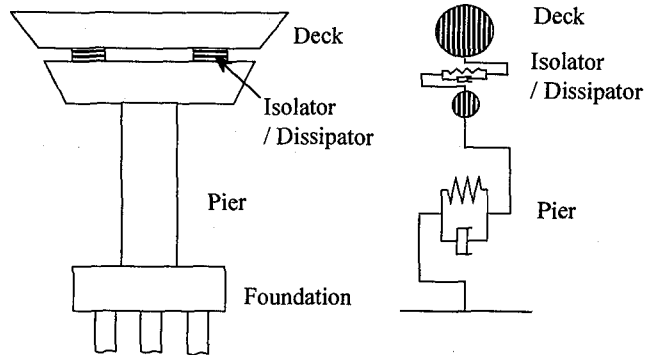


Fig. 4 Analytical Model of an Isolated Bridge

and 3. It should be noted in Figs. 2 and 3 that the lateral force is defined at the gravity center of the deck. Two types of isolator/energy dissipators are considered here for analysis. The first is the sliding-type isolator with zero post-yield stiffness, and the other is the lead-rubber bearings (LRB) and high damping rubber bearings (HDR) which have positive post-yield stiffness. In such devices, the level of yield force  $P_y^b$  may be a controlling factor for the bridge response. It is obvious that the yield force of the device  $P_y^b$  should be less than the yield force of the pier  $P_y^p$  to achieve favorable response reduction in seismic isolation. It is anticipated that the nonlinear interaction between the device and the pier depends on the yield force ratio  $P_y^b / P_y^p$ .

Assuming that the soil is stiff, the response of bridge may be idealized as a two-degree-of-freedom system as shown in Fig. 4. The lateral force vs. lateral displacement hysteresis of the pier and the device is idealized as the bilinear hysteresis models for simplicity of the analysis. Considering a reinforced concrete bridge pier with 10m high, 2.2m deep in longitudinal direction and 5m wide in transverse direction, the cracked stiffness  $k_i^p$  and the yield force of the pier  $P_y^p$  are assumed as 94800 kN/m and 3000 kN, respectively.

The initial stiffness of the devices is assumed here as 47400 kN/m. This corresponds to the LRB and HDR with 200mm high and 650mm diameter. The post-yield stiffness

of LRB and HDR is assumed as 7290 kN/m, which is 1/6.5 of the initial stiffness<sup>7)</sup>.

It is also assumed that the mass of deck is 1000ton (weight = 9800 kN) and that the mass of the pier is 1/5 of the mass of the deck. Thus the bridge has the fundamental natural period of 0.71 second. Damping ratio of 2 % is assumed for the pier and the device. Hysteretic damping is further considered for the device in the nonlinear analysis. After modal damping ratios are computed based on the strain-proportional method<sup>4)</sup>, two coefficients of the Rayleigh damping are determined.

Three ground accelerations which were spectrally fitted to a design response spectrum are used for the analysis. The design response spectrum for the Type I ground motion at Soil Group III (soft soil site) is considered here. Spectral fitting was conducted by varying the amplitude of ground acceleration with the phase angle being unchanged<sup>8)</sup>. Fig. 5 shows the three ground accelerations thus generated.

### 3. Response of Bridges Isolated by the Device with Zero Post-Yield Stiffness

Fig. 6 shows the lateral force vs. lateral displacement hysteresis of the pier and the device for typical combinations of the yield force of pier  $P_y^p$  and the yield force of the device  $P_y^b$ . As anticipated, the pier response decreases

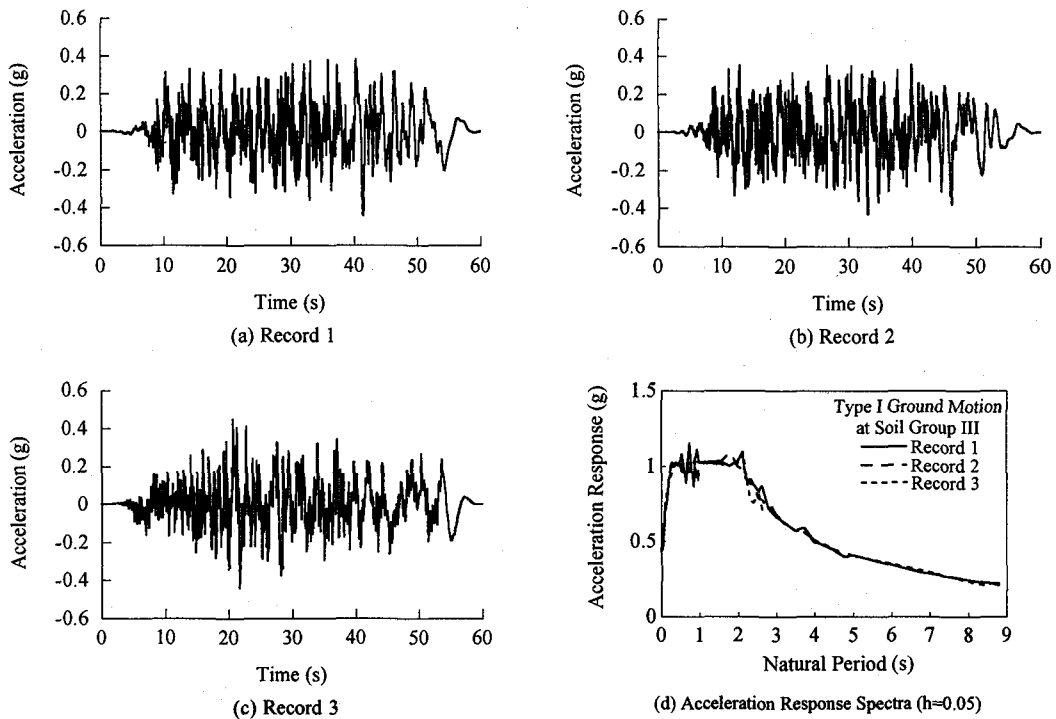


Fig. 5 Ground Accelerations used for Analysis and Response Spectra ( $h=0.05$ )

and the device response increases as the yield force ratio  $P_y^b / P_y^p$  decreases. Fig. 7 shows how the responses of the pier and the device vary as the yield force ratio  $P_y^b / P_y^p$  changes. The responses of the pier and the device are represented in terms of the ductility factor defined as

$$\mu^p = u_{\max}^p / u_y^p \quad (2)$$

$$\mu^b = u_{\max}^b / u_y^b \quad (3)$$

in which  $u_{\max}$  and  $u_y$  represent the peak and the yield displacement, respectively. The superscripts b and p denote the device and the pier, respectively.

Although the results for three ground motions are presented in Fig. 7, they are almost the same. It is important in Fig. 7 that the pier response reduces for  $P_y^b / P_y^p$  smaller than 1.4, but that nonlinear response of the pier occurs at  $P_y^b / P_y^p$  as small as 0.2. Finally at  $P_y^b / P_y^p$  of about 0.1, the pier response becomes elastic. Because the weight of the deck which is laterally supported by the pier is 9800 kN, this means that the linear response of pier can be achieved when the yield force of the device  $P_y^b$  is less than 3 % of the deck weight (9800kN). Since it is difficult to design the yield force of the device  $P_y^b$  less than 3 % of the deck weight generally, the nonlinear response of the pier is inevitable.

To evaluate the degree of nonlinear deformation of the pier and the device, the total energy dissipation was evaluated as

$$W^p = \oint P^p du^p \quad (4)$$

$$W^b = \oint P^b du^b \quad (5)$$

in which  $W^p$  and  $W^b$ : the total energy dissipated in the pier and the device, respectively,  $P^p$  and  $P^b$ : restoring force developed in the pier and the device, respectively, and  $u^p$  and  $u^b$ : lateral displacement of the pier and the device, respectively. The total energy of the bridge is then evaluated as

$$W = W^p + W^b \quad (6)$$

To represent the damage degree of the pier, a parameter  $r^p$  defined by Eq. (7) is introduced.

$$r^p = \frac{W^p}{W} \quad (7)$$

The  $r^p$  is designated hereinafter as the damage ratio parameter.

Fig. 8 shows the total dissipated energy  $W^p$  and  $W^b$  as well as the damage ratio parameter  $r^p$ . While the total dissipated energy in the pier and the device is smaller for the record 3 than the record 1 and 2, the damage ratio parameter  $r^p$  is almost free from the difference of ground accelerations. It is seen in Fig. 8 (a) that the total dissipated energy in the pier  $W^p$  decreases and, on the contrary, the total dissipated energy in the device  $W^b$  increases as the yield force ratio  $P_y^b / P_y^p$  decreases from about 1.4. Such relation is similar to Fig. 7. The only difference from Fig. 7 is that  $W^b$  in Fig. 8 (a) starts to decrease again at  $P_y^b / P_y^p$  less than 0.6. This may be understood from Fig. 9. Although the peak displacement

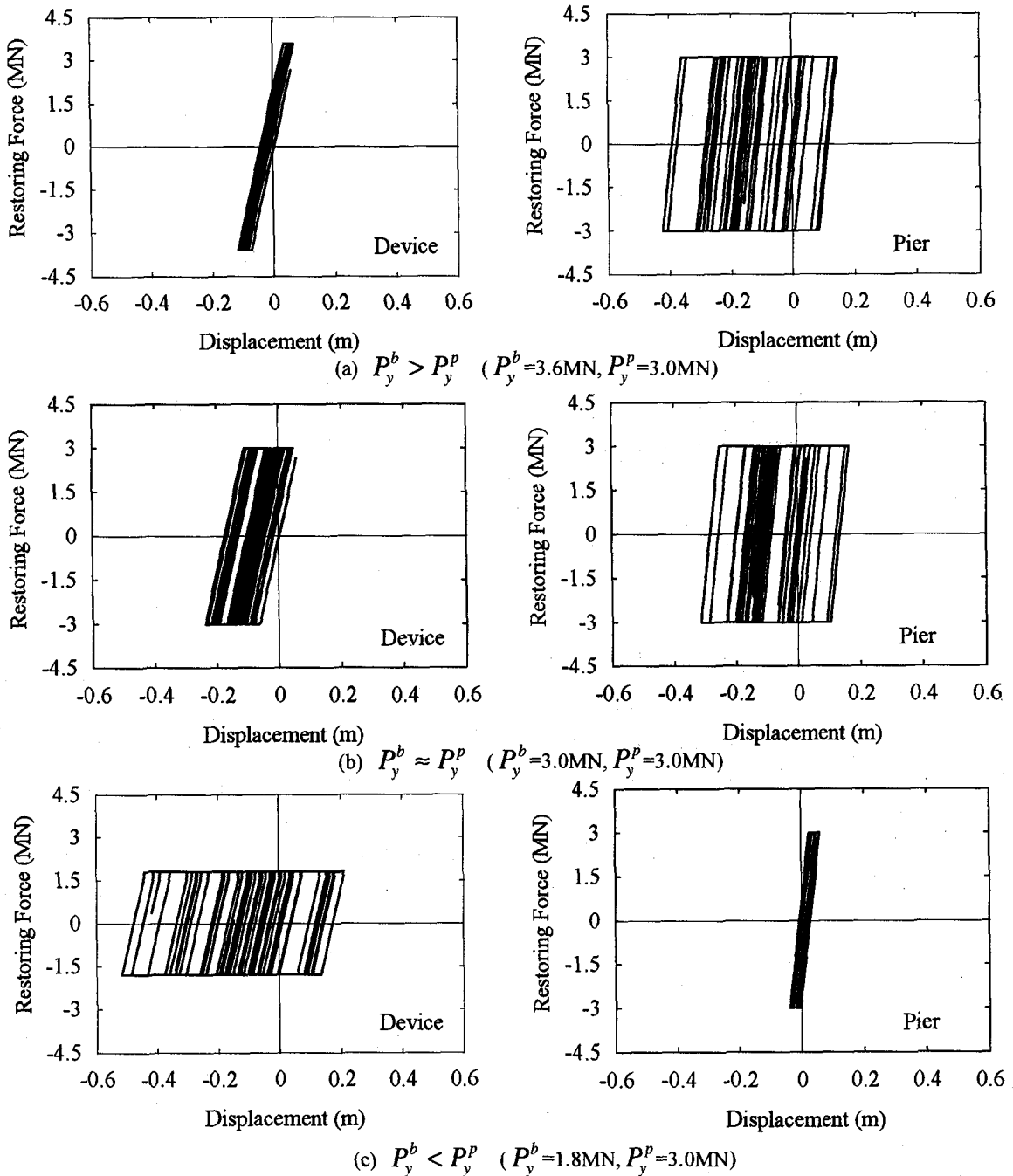


Fig. 6 Lateral Force vs. Lateral Displacement Hysteresis for Pier and Device  
(Device with Zero Post-Yield Stiffness)

of the device  $u^b$  increases as the yield force ratio  $P_y^b / P_y^p$  decreases, the total amount of energy dissipated in the device decreases.

#### 4. Response of Bridges Isolated by the Device with Positive Post-Yield Stiffness

Similarly, the nonlinear interaction between the device and the pier was analyzed for the bridge isolated by the device with positive post-yield stiffness. Fig. 10 shows the

lateral force vs. lateral displacement hysteresis of the pier and the device. Although the general trend that the total energy dissipated in the pier decreases as the yield force ratio  $P_y^b / P_y^p$  decreases is the same with the bridge isolated by the device with zero post-yield stiffness, it is important to note that the total energy dissipated in the pier starts to increase at small yield force ratio as shown in Fig. 10 (d). This is because the small yield force of the device  $P_y^b$  results in the increase of displacement of the device, and this in turn causes that the peak lateral force induced in the device

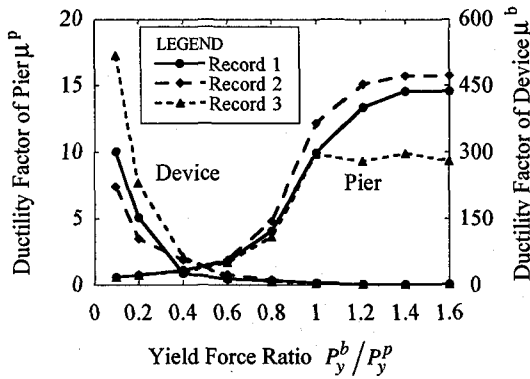
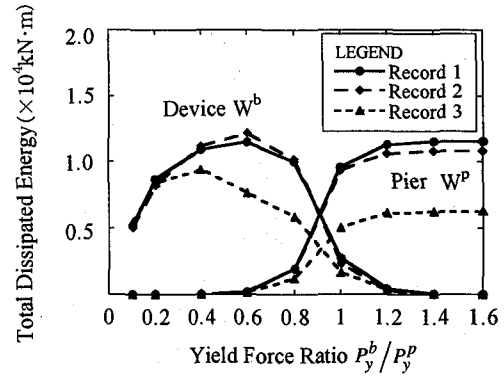
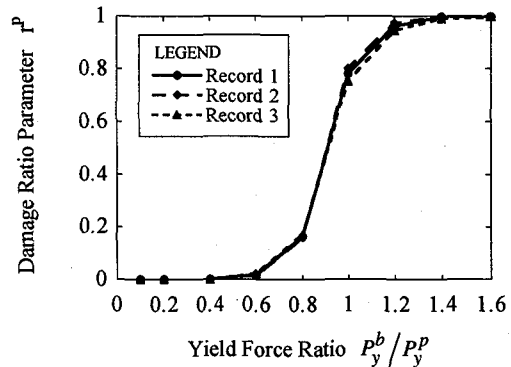


Fig. 7 Effect of the Yield Force of the Pier and the Device  $P_y^p$  and  $P_y^b$ , on the Ductility Factor of the Pier and the Device (Device with Zero Post-Yield Stiffness)

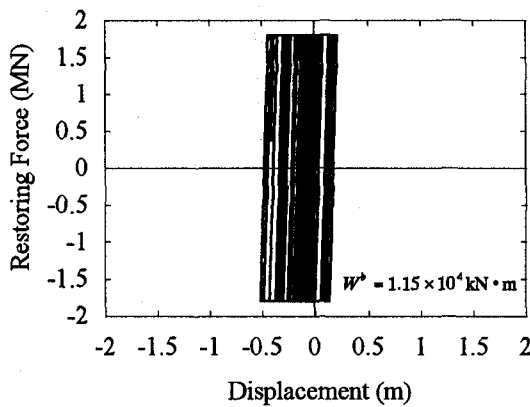


(a) Total Dissipated Energy

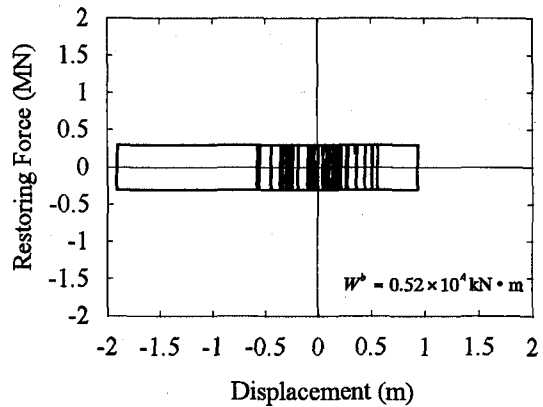


(b) Damage Ratio Parameter  $r^p$

Fig. 8 Effect of the Yield Force of the Pier and the Device  $P_y^p$  and  $P_y^b$ , on the Damage Degree (Device with Zero Post-Yield Stiffness)



(a)  $P_y^b < P_y^p$  ( $P_y^b = 1.8\text{MN}$ ,  $P_y^p = 3.0\text{MN}$ )



(b)  $P_y^b \ll P_y^p$  ( $P_y^b = 0.3\text{MN}$ ,  $P_y^p = 3.0\text{MN}$ )

Fig. 9 Energy Dissipated in the Device with Small Yield Force  $P_y^b$

exceeds the yield force of the pier  $P_y^p$ .

Figs. 11 and 12 show the dependence of the ductility factor, the total dissipated energy and the damage ratio parameter on the yield force ratio. It is seen that the total dissipated energy of the pier  $W^p$  and the damage ratio parameter  $r^p$  start to increase at  $P_y^b / P_y^p$  less about 0.4. This is unique characteristics of the device with positive post-yield stiffness, and has to be carefully considered in design.

It should be noted here that the ductility factor of the

device  $\mu^b$  with positive post-yield stiffness is much smaller than that with zero post-yield stiffness (refer to Figs. 7 and 11). This is obviously the effect of increasing the lateral force of the device as the deformation increases. The positive post-yield stiffness of the device prevents the build-up of the deformation of the device while it does not bring the sharp decrease of the pier ductility factor  $\mu^p$  as was the case in the bridge with zero post-yield stiffness.

It is common to set the yield force of the device  $P_y^b$  at

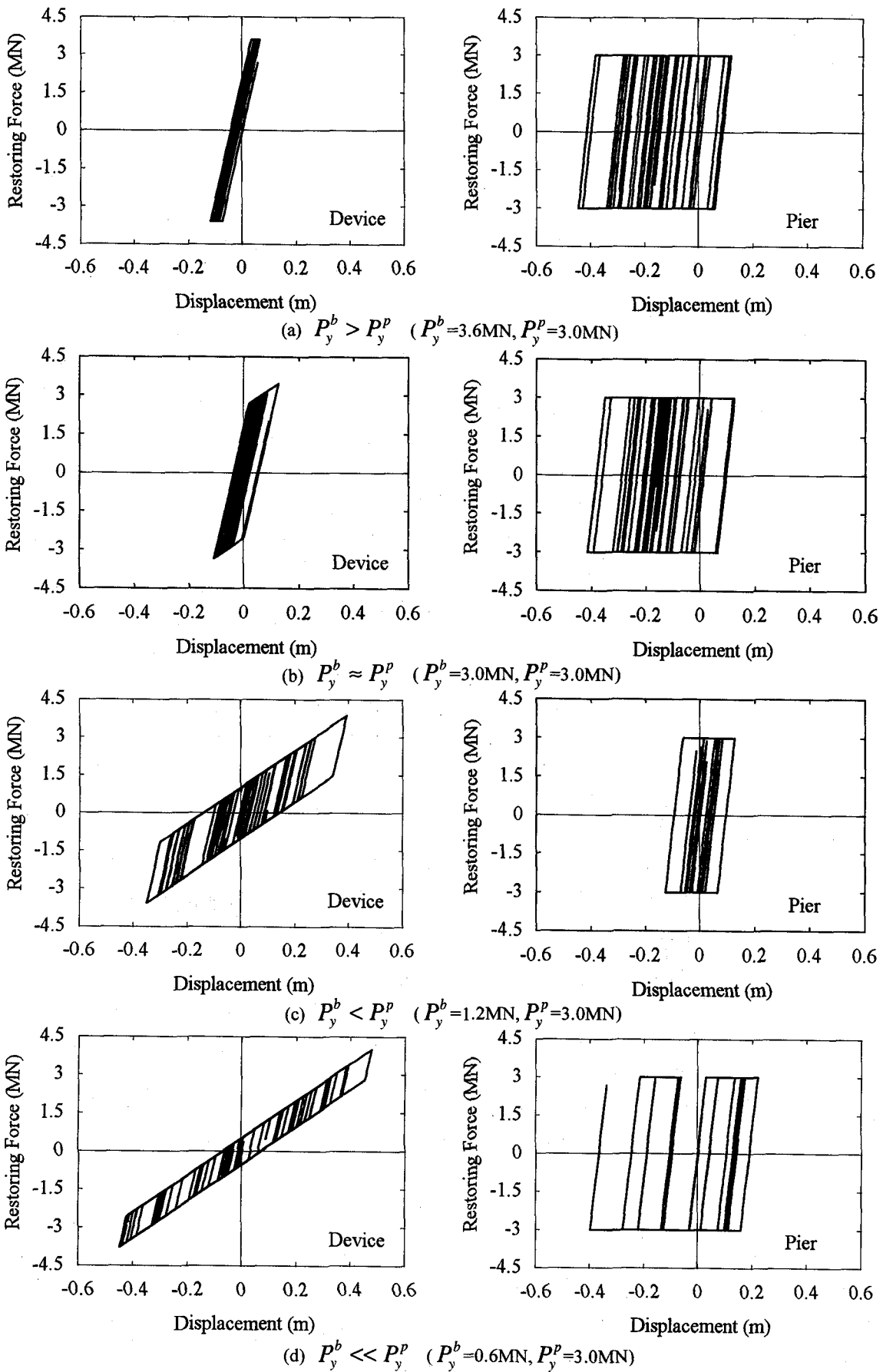


Fig. 10 Lateral Force vs. Lateral Displacement Hysteresis for Pier and Device  
(Device with Positive Post-Yield Stiffness)

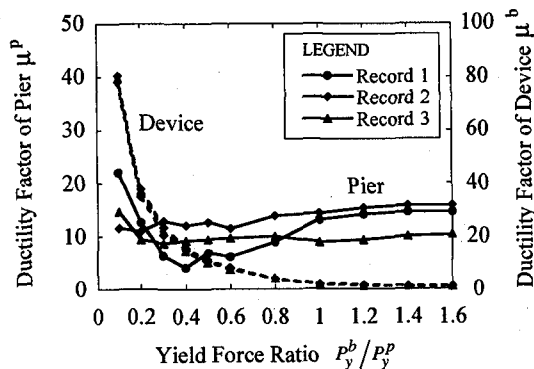
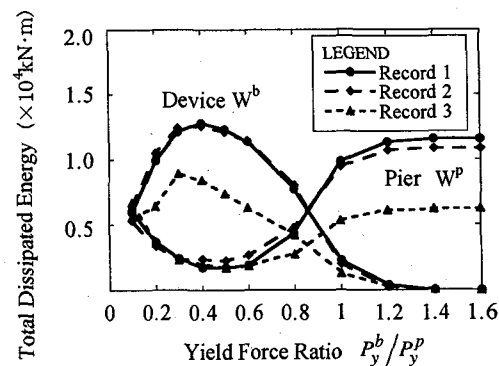
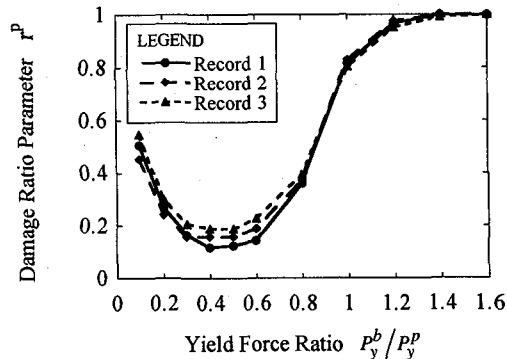


Fig.11 Effect of the Yield Force of the Pier and the Device  $P_y^P$  and  $P_y^b$ , on the Ductility Factor of the Pier and the Device (Device with Positive Post-Yield Stiffness)



(a) Total Dissipated Energy



(b) Damage Ratio Parameter  $r^P$

Fig.12 Effect of the Yield Force of the Pier and the Device  $P_y^P$  and  $P_y^b$ , on the Damage Degree (Device with Positive Post-Yield Stiffness)

about 0.1 ~ 0.2 of the deck weight. This corresponds to the yield force ratio  $P_y^b / P_y^P$  of 0.3 ~ 0.6. It is seen in Figs. 7 and 8 that this yield force level is appropriate in design.

### 5. Elongation of Natural Period for Isolation

From the peak response of the pier and the device, the equivalent stiffnesses of the pier and the device,  $K_e^P$  and  $K_e^b$ , may be evaluated as shown in Fig. 13<sup>3)</sup>. The fundamental natural period of the bridge (pier-device-deck system) may be computed as

$$T = 2\pi \sqrt{\frac{W}{g \cdot K_e}} \quad (8)$$

in which  $K_e$  is the effective stiffness of the bridge, and is given as

$$K_e = \frac{K_e^P \cdot K_e^b}{K_e^P + K_e^b} \quad (9)$$

Fig. 14 (a) shows the natural period  $T$  vs. total energy dissipated in the pier  $W^P$  relation for the bridge isolated by the device with positive post-yield stiffness. It is seen in Fig. 14 (a) that the total dissipated energy of the pier  $W^P$  sharply decreases as the natural period  $T$  increases from 2 second. Because of the flexibility of device, natural period of the bridges is longer than 2 second in all cases. It should

be noted that the data at natural period longer than 2.5 second corresponds to the bridges isolated by the device with low yield forces. Therefore the larger response displacement of the devices with low yield force results in the larger energy dissipation in the pier.

When the deck is supported by the normal bearing, the natural period of the bridge is

$$T_f = 2\pi \sqrt{\frac{W}{g \cdot K_e^P}} \quad (10)$$

and the energy dissipation of the bridge is

$$W_f = \oint P_f^P du_f^P \quad (11)$$

in which  $P_f^P$  and  $u_f^P$  are the lateral force and the lateral displacement of the pier when the deck is supported by the normal bearing.

In Fig. 14 (b), natural period  $T$  and the total energy dissipated in the pier  $W^P$  are normalized by  $T_f$  and  $W_f$ , respectively. Because  $T_f$  and  $W_f$  are constant, the shape of Fig. 14 (b) is the same with that of Fig. 14 (a). If it is considered that the use of device is favorable at  $W^P / W_f$  less than 1.0, natural period of the isolated bridge  $T$  should be longer than 2 second, which corresponds to  $T / T_f$  of about 3.

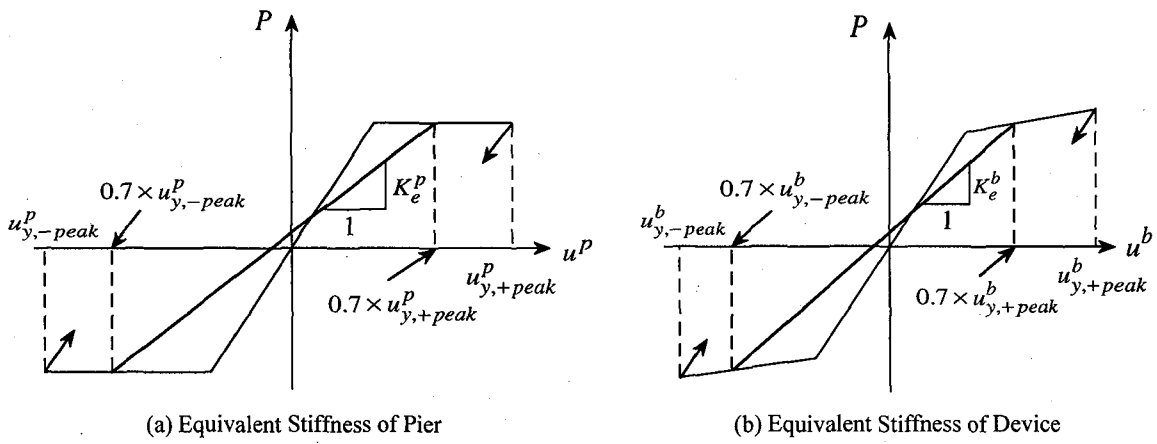


Fig.13 Definition of Equivalent Stiffness of Pier and Device

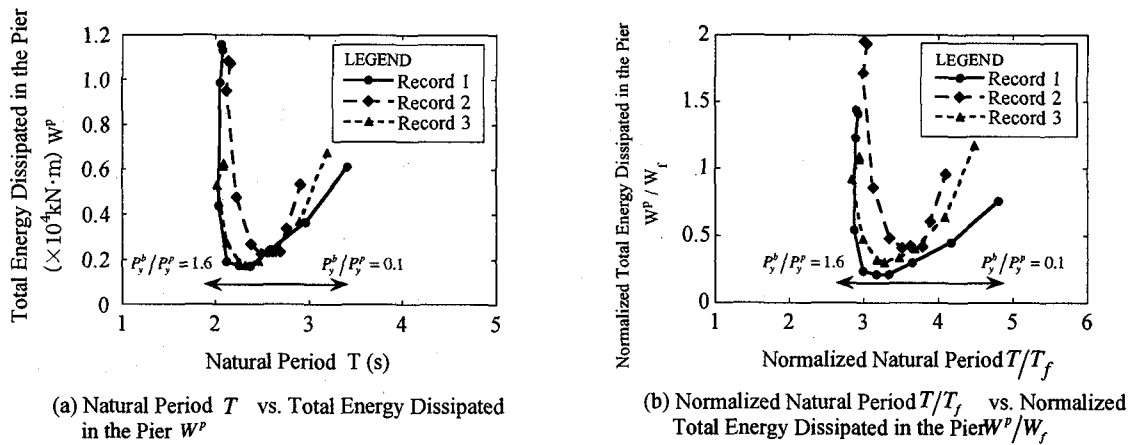


Fig. 14 Dependence of Total Energy Dissipated in the Pier on the Natural Period (Device with Positive Post-Yield Stiffness)

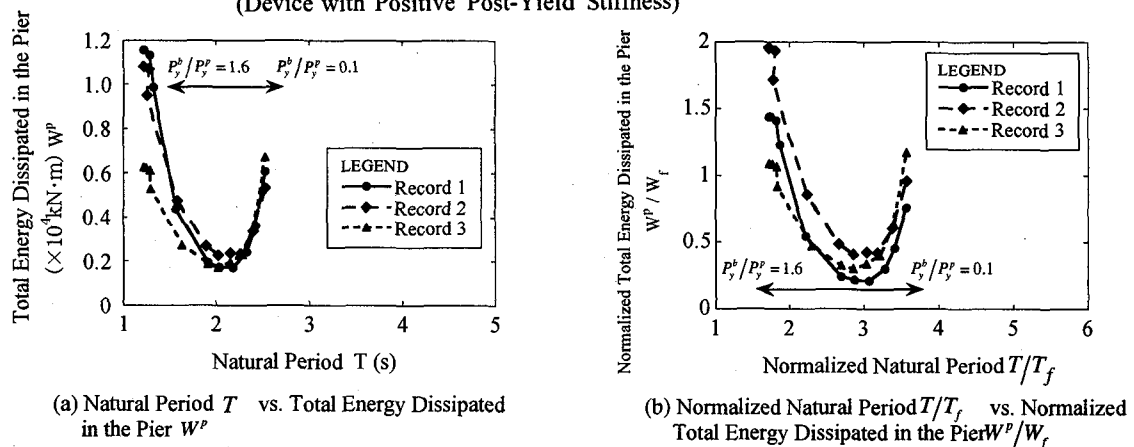
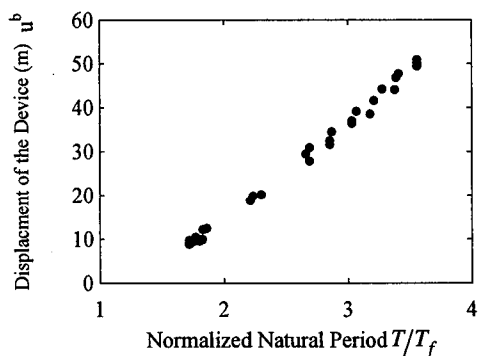


Fig. 15 Dependence of Total Energy Dissipated in the Pier on the Natural Period computed with use of Cracked Stiffness of the Pier (Device with Positive Post-Yield Stiffness)

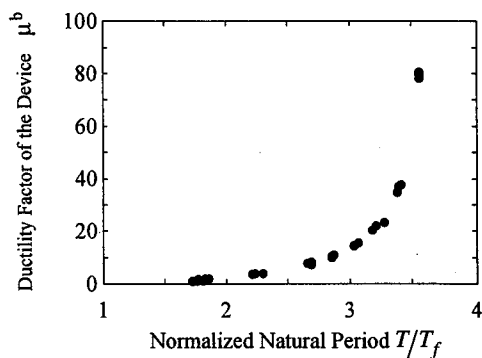
As previously described, it is recommended in the Design Specification of Highway Bridges that natural period of a menshin bridge may be about 2 times the natural period of non-menshin bridges. However, it is assumed in the Specification that natural periods of both menshin bridge and non-menshin bridge are computed with use of the cracked stiffness of the pier. Because the equivalent stiffness of the pier depending on the peak response displacement as shown

in Fig. 13 (a) is used in Fig. 14, the  $W^p/W_f$  vs.  $T/T_f$  relation was computed using the cracked stiffness of the pier following the procedure of the Design Specifications. This result is shown in Fig. 15. It is observed that  $T/T_f$  of 2 is appropriate to reduce the response of the bridges. Although further elongation of the natural period reduces the energy dissipation of the pier, it brings larger response of the deck as shown in Fig.16. It should be noted that because the





(a) Normalized Natural Period  $T/T_f$  vs. Displacement of the Device  $u^b$



(b) Normalized Natural Period  $T/T_f$  vs. Ductility Factor of the Device  $\mu^b$

Fig. 16 Displacement of the Device vs. Natural Period computed with use of Cracked Stiffness of the Pier (Device with Positive Post-Yield Stiffness)

ground motions which decrease the response spectral amplitude at the natural period longer than 2.0 second were used in this analysis, the appropriateness of the  $T/T_f$  of 2 needs to be studied for other types of ground motions.

## 6. Conclusions

A series of analysis was conducted for a menshin bridges to clarify the yield force of the device. From the analysis presented herein, although the types of ground motions and the structural characteristic are limited, the following conclusions may be deduced:

- (1) When the device with zero post-yield stiffness is used, the ductility factor of and energy dissipation of the pier decrease as the yield force ratio  $P_y^b / P_y^p$  decreases from 1.4. However, even at  $P_y^b / P_y^p$  less than 0.4, hysteretic response occurs in the pier, and  $P_y^b / P_y^p$  has to be less than 0.1 for making the pier response elastic.
- (2) Although the general trend is the same with (1) for the bridges isolated by the device with positive post-yield stiffness, the ductility factor of and the energy dissipated in the pier are large at  $P_y^b / P_y^p$  less than about 0.4. This is because large nonlinear response occurs in the device when the yield force  $P_y^b$  is small, and this results in the lateral force in the device larger than the yield force of the pier  $P_y^p$ . Thus, the yield force of the device has to be carefully evaluated in design.
- (3) About two times the natural period of a bridge supported by the normal bearing may be an appropriate estimation for the natural period of a menshin bridge isolated by the device with positive post-yield stiffness.

## References

- 1) Technical Research Center for National Land

Development: Guidelines for Menshin Design of Highway Bridges, 1993.

2) Kawashima, K.: Manual for Menshin Design of Highway Bridges, Proc. 2nd US-Japan Workshop on Earthquake Protective Systems of Bridges, Technical Memorandum No. 3196, pp. 195-219, Public Works Research Institute, Tsukuba, Japan, 1992.

3) Ministry of Construction: Manual of Menshin Design of Highway Bridges, Technical Note, No. 60, Public Works research Institute, 1993. English translation is available by Sugita, H. and Mahin, S.: Manual for Menshin Design of Highway Bridges: Ministry of Construction, Japan, Report No. EERC 92-10, Earthquake Engineering Research Center, University of California, Berkeley, USA, 1994.

4) Japan Road Association: Design Specifications of Highway Bridges, 1996.

5) For example, Kawashima, K., Hasegawa, K. and Nagashima, H. : A Perspective of Menshin Design of Highway Bridges in Japan, Proc. First US-Japan Workshop on Earthquake Protective Systems for Bridges, Technical Report NCEER 92-4, pp. 3-25, National Center for Earthquake Engineering, State University of New York at Buffalo, USA, 1992.

6) Priestley, M.J.N., Seible, F. and Calvi, G.M.: Seismic Design and Retrofit of Bridges, John Wiley & Sons, USA, 1996.

7) Skinner, I., Robinson, W. H. and McVerry, G. H.: An Introduction to Seismic Isolation, John Wiley & Sons, USA, 1993.

8) Arakawa, T., Kawashima, K. and Aizawa, K.: Spectral Fitting Method for Generating Ground Motion for Dynamic Response Analysis, Civil Engineering Journal, Vol. 26-7, pp. 392-397, 1984.

(Received September 26, 1997)